JOURNAL OF MATERIALS SCIENCE 31 (1996) 499–506

Relation between axial compressive strength of reinforcing fibres and fibre diameter

M. MIWA, Y. LIU, H. TSUZUKI, A. TAKENO, A. WATANABE
Faculty of Engineering, Gifu University, Yanagido 1-1, Gifu, Japan 501-11

Attempts were made to estimate the fibre axial compressive strength of pitch-based graphitized and polyarylate fibres, and the relationship between the compressive strength and fibre diameter was investigated. The estimated compressive strength of fibres decreases with increasing temperature. This decrease in compressive strength may be accounted for by a decrease in the radial compressing force. There is a linear relationship between the estimated compressive strength and radial compressing force in a temperature range from room temperature to 80 °C. The real compressive strength of the fibres, determined by extrapolating this straight line until the radial compressing force is zero, increases with decreasing fibre diameter, but remains almost unchanged at a diameter range smaller than 10 μm. In order to obtain reinforcing fibres having a higher compressive strength, it will be necessary to prepare fibres having a diameter smaller than 10 μm.

1. Introduction

The relation between the mechanical properties of composites in tension and those of the fibres used as reinforcements has been studied both experimentally and theoretically in fairly great detail. However, in spite of the fact that the compressive characteristics of composites depend on the characteristics of reinforcing fibres, there has been almost no study on the mechanical properties of composites in compression. Several attempts to determine the compressive characteristics of reinforcing fibres have been made by (1) the elastic loop test [1–4], (2) the bending beam test [5–10], (3) a test based on fibres embedded in a matrix [11–14], (4) the recoil test [15–19], and, [5] a test based on compressive strength of composites [20–22], but there is still no decisive method. Compressive strengths of various reinforcing fibres obtained from these test methods have been compared by Kumar and Helminiak [23–25].

We have reported a method for measuring the compressive strength of fibres in which, if a sufficiently long fibre is embedded in the neighbourhood of the surface of a rectangular beam and the system is subjected to a tensile (or compressive) strain rather than a fibre ultimate strain according to the bending method, the fibre eventually breaks into many pieces. By measuring the lengths of the broken pieces, the axial compressive strength of the fibre can be estimated in both cases where the tensile strength of the fibres is assumed to be uniform [26, 27] and where it is assumed to be variable [28, 29]. Using the latter method, we estimated the compressive strengths of carbon and aramid fibres. It was found that the estimated compressive strength of PAN-based carbon fibres was higher than pitch-based fibres, and that of carbonized fibres (higher strength type) was higher than that of graphitized fibres (higher modulus type) [26, 27, 29, 30]. Moreover, the axial fibre compressive strength was approximately 10%–60% of the tensile strength [29], and it increased with increasing degree of orientation or face spacing of the crystal. In addition, it increased with decreasing crystal size [30]. Furthermore, it was only 2%–3% of the tensile strength for aramid fibres, due to the formation of kink bands [28].

It is generally known that the tensile strength of brittle fibres, such as carbon, glass, aramid and polyarylate fibres, is variable with fibre size, i.e. it decreases as the length or diameter of the fibre increases. Accordingly, it is expected that the compressive strength of reinforcing fibres is variable with fibre diameter. However, there have been no studies of the effect of fibre diameter on the compressive strength of reinforcing fibres.

In this work, the relationship between the fibre diameter and the compressive strength for carbon and polyarylate fibres was investigated using our method as described in previous papers [27, 28] in which the tensile strength of fibres was taken into consideration.

2. Experimental procedure

The fibres used were three kinds of pitch-based graphitized fibres (higher modulus type, experimental samples of Tonen) and four kinds of polyarylate fibres (Vectran, higher strength type, experimental samples of Kuraray). Their respective diameters are shown in Table I.

First, tensile tests were performed using 5, 25, 40, and 100 mm gauge lengths to obtain distribution curves of tensile strength for the fibres. The instrument used was a Tensilon UTM-I-2500 type (Orientec),

0022–2461

TABLE I Mechanical properties of fibres (at 20° C, test length 25 mm)

Fibre	Carbon			Polyarylate			
	C-1	C-2	C-3	V-1	V-2	V-3	V-4
Diameter (μm)	7.2	10.0	13.8	12.2	17.4	22.9	29.3
Tensile strength (GPa)	3.21	2.64	2.35	3.93	3.47	3.34	3.62
Young's modulus (GPa)	509	526	524	79.6	75.7	74.8	73.5
Breaking strain (%)	0.72	0.61	0.52	0.41	0.40	0.38	0.39

strain rate 0.05 mm mm^{-1} min^{-1}, and the number of fibres tested was 100 pieces for each gauge length. The results obtained by the fibre tensile strength distribution tests were used to determine Weibull parameters.

Second, rectangular specimens were prepared for measuring fragment length under the same conditions as reported in preceding papers [26–30]. Epoxy resin (Epikote 828, Yuka Shell), 100 parts, was mixed with 10 parts of an amine-hardening agent (S-Cure 661, Kayaku Nuri). The mixture was agitated thoroughly and then defoamed. This mixture was poured into a mould holding a fibre at a constant tension in the neighbourhood of the surface of a rectangular specimen and subjected to curing at 65° C for 17 h.

The specimens prepared in this manner were submitted to measurement of fragment length, i.e. each specimen was subjected to a tensile (or compressive) strain of 4% at a drop rate of the upper heads of 10 mm min^{-1} using the four-point bending method under the same conditions as reported in preceding papers [26–30].

As indicated elsewhere [27], the fibre buckles at a temperature range higher than 100° C. Accordingly, in this experiment, to investigate the effect of a radially compressing force on the fibre axial compressive strength, measurements were made at 20–100 °C. Over 200 fragments were examined for each experimental condition.

3. Results and discussion

The typical strength distributions of graphitized and polyarylate fibres used in this experiment are shown in Figs 1 and 2, respectively.

The tensile strength of brittle fibres, such as carbon fibres, is generally affected by partial flaws. In general, the tensile strength of such fibres is represented by a chain model. This model represents a fibre by a chain consisting of n pieces of equal links. Applying the Weibull distribution function, probability $g(\sigma)$ in which a chain of n links will break at stress σ can be expressed as [31, 32]

$$g(\sigma) = nm\sigma_o^{-1}\left(\frac{\sigma-\sigma_p}{\sigma_o}\right)^{m-1}\exp\left[-n\left(\frac{\sigma-\sigma_p}{\sigma_o}\right)^m\right] \quad (1)$$

where m, σ_o and σ_p are the Weibull parameters. Also, the mean tensile strength $(\bar{\sigma}_{f,L})_t$ of the fibre at length L is given as [31, 32]

$$(\bar{\sigma}_{f,L})_t = \sigma_p + \left[\frac{\sigma_o}{(L/l_l)^{1/m}}\right]\Gamma\left(\frac{m+1}{m}\right) \quad (2)$$

where Γ is the complete gamma function. l_l is the length of link (gauge length L/number of the links) consisting of the fibres.

The solid lines in Figs 1 and 2 represent theoretical values obtained by substituting Weibull parameters m, σ_o and σ_p and the length of links l_l given in Table II, into Equation 1. An example of the comparison of the experimental mean tensile strengths with ones calculated by Equation 2 is shown in Table III. The relationship between the logarithm of gauge length and the logarithm of the mean tensile strength is also shown in Fig. 3. The solid lines in Fig. 3 represent theoretical values calculated by substituting Weibull parameters and the length of links into Equation 2. The theoretical values obtained by Equations 1 and 2 employing the values of Weibull parameters and the length of links given in Table II, agree with the measured values. Therefore, the values of Weibull parameters and the length of links thus determined are appropriate. Moreover, the constant value of mean tensile strength within the range of shorter gauge length in Fig. 3 shows that the tensile strength of fibre is uniform in the length range shorter than the link length.

In preceding papers [28, 29], when variable tensile strength of the fibre is assumed, the mean axial compressive strength $(\bar{\sigma}_f)_c$ of fibre is given by

$$(\bar{\sigma}_f)_c = (\bar{\sigma}_{f,L})_t\frac{(\bar{l})_c}{(\bar{l})_t} \quad (3)$$

where $(\bar{\sigma}_{f,L})_t$ is the mean tensile strength of the fibre at length L and is given by the above-mentioned Equation 2; $(l)_c$ is the mean fragment length in compression, and, $(\bar{l})_t$ is the mean fragment length in tension.

The photographs of fibre fragments of the specimen compressed by the above-mentioned procedure are shown in Fig. 4. The fibre is broken into a number of fragments. Many kink bands can be observed in polyarylate fibres, in the same manner as the fracture of aramid fibres [28].

The relationship between both the mean fragment length $(\bar{l})_t$ in tension and $(\bar{l})_c$ in compression of composite systems including reinforcing fibres having tensile strength distributions and temperature, are shown in Figs 5 and 6, respectively. For polyarylate fibres, the distance between the kink bands was considered as the fragment length.

When all the fragments have been reduced to less than the critical fibre length, no further elongation of the specimen will cause the fibre to break. When the

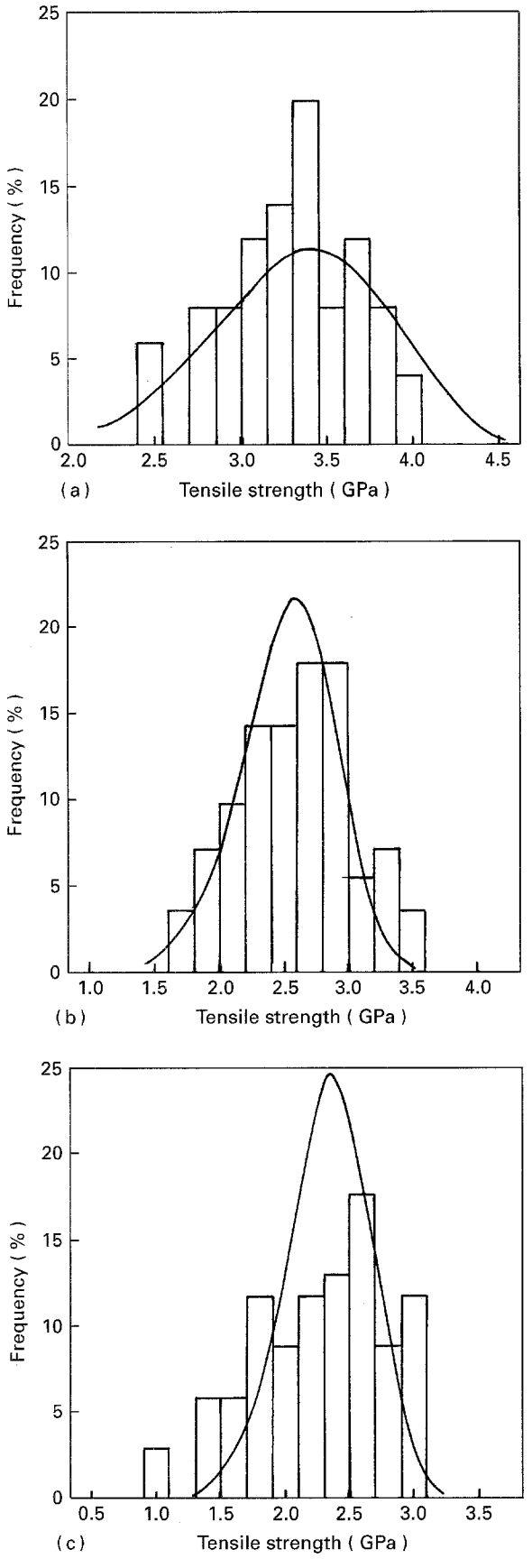

Figure 1 Strength distribution of graphitized fibres (test length 25 mm). (a) C-1 fibre, (b) C-2 fibre, (c) C-3 fibre. See Table I for the sample descriptions.

fibre finally breaks into many pieces, we have previously proposed that this considerable tensile strength is the tensile strength at the length just before the final fragment lengths [32].

If $\bar{l}$ represents the average value of final fragment length, $K\bar{l}$ the first embedded length, and $k\bar{l}$ the length just before the length $\bar{l}$, then, the average value $\bar{L}^*$ of length just before the fragment length with $\bar{l}$ is given by [32]

$$\bar{L}^* = \frac{4}{3}\bar{l} + \sum_{k=3}^{K-1} k\bar{l}\left(\frac{4}{k-1}\right)\left(\frac{1}{3}\right)^{k-1} + K\bar{l}\left(\frac{2}{K-1}\right)\left(\frac{1}{3}\right)^{K-2} \tag{4}$$

The average value, $\bar{L}^*$, of the length just before the length $(\bar{l})_t$ from the mean fragment length $(\bar{l})_t$ (Fig. 5) in tension according to Equation 4, can also be calculated. Furthermore, the mean tensile strength $(\bar{\sigma}_{f,L})_t$ of fibres is determined by substituting the value $\bar{L}^*$ into Equation 2 using a method described in previous papers [28, 29, 32].

Fig. 7 shows the relationship between the mean value of fibre axial compressive strength $(\bar{\sigma}_f)_c$, estimated from the mean fragment length $(\bar{l})_t$ (Fig. 5) in tension, the mean fragment length $(\bar{l})_c$ (Fig. 6) in compression, and the mean tensile strength $(\bar{\sigma}_{f,L})_t$ of the fibre according to Equation 3, and temperature. With these systems, in the same manner as observed in carbon and aramid fibres [26–30], the estimated compressive strength decreases with increasing temperature up to 80 °C. As indicated elsewhere [26–29], it is conceivable that the radial force compressing the fibre, decreased by both the decrease in residual thermal stress and Young's modulus of the resin matrix with increasing temperature, may cause a temperature dependence of the estimated value of the fibre axial compressive strength.

The estimated compressive strength increases greatly above 80 °C. It is conceivable that the fibre buckles, and the conditions for application of Equation 3 cannot be satisfied above 80 °C [26–29]. Accordingly, further details are discussed for results obtained at a temperature range lower than 80 °C.

When a fibre is embedded in the resin and the system is allowed to cure, the thermal stress, $(P)_T$, working perpendicular to the fibre–resin interface, is approximately given by the following equation [33]

$$(P)_T = \frac{(\alpha_m - \alpha_f)\, E_m \Delta T}{1 + \nu_m} \tag{5}$$

where α is the thermal expansion coefficient, E is Young's modulus, ν is Poisson's ratio, ΔT is the difference in temperature from the moulding temperature, and the subscripts m and f denote matrix and fibre, respectively. Fig. 8 shows the relationship between the thermal stress, $(P)_T$, obtained by Equation 5 and temperature. The thermal expansion coefficient, α_m, Young's modulus, E_m, and Poisson's ratio, ν_m, required to calculate thermal stress, are shown in Table IV. We have utilized a thermal expansion coefficient α_f perpendicular to the fibre axis, where α_f is $9.9 \times 10^{-6}\,°C^{-1}$ [34] for graphitized fibre, and $3.3 \times 10^{-6}\,°C^{-1}$ [35] for polyarylate fibre. In addition, we have assumed that these values were constant in the temperature range of this experiment.

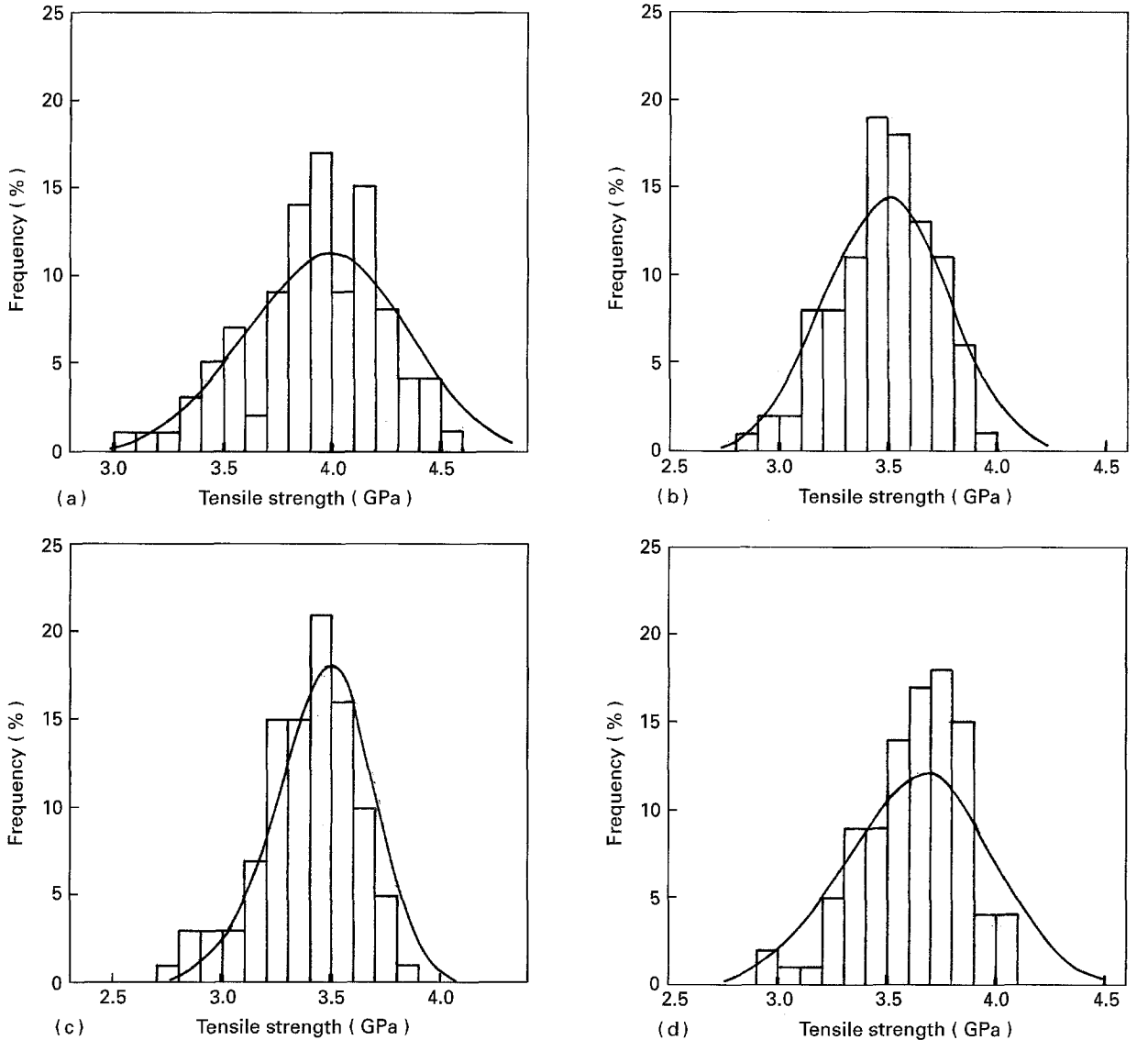

Figure 2 Strength distribution of polyarylate fibres (test length 25 mm). (a) V-1 fibre, (b) V-2 fibre, (c) V-3 fibre, (d) V-4 fibre. See Table I for the sample descriptions.

TABLE II Statistical values of tensile strength for fibres

Fibre	m	σ_o (GPa)	σ_p (GPa)	Length of links l_l (mm)
Carbon				
C-1	5.3	4.69	0.98	1.025
C-2	5.8	4.24	0.69	0.30
C-3	4.8	4.03	0.98	0.20
Polyarylate				
V-1	4.0	4.53	2.73	0.21
V-2	3.6	3.96	2.62	0.16
V-3	5.2	3.68	2.47	0.042
V-4	4.1	4.69	2.47	0.13

Fig. 9 shows the relationship between the estimated mean compressive strength $(\bar{\sigma}_f)_c$ (Fig. 7) and the thermal stress $(P)_T$ (Fig. 8) obtained through the function of temperature. With these fibre diameters, the estimated mean compressive strength of graphitized and polyarylate fibres decreases linearly with decreasing thermal stress.

As indicated in previous papers [26–30], it is conceivable that the real compressive strength of fibres is the strength when the radial compressing force, i.e. the residual thermal stress in this experiment, is zero. Accordingly, we have considered the value obtained by extrapolating the straight line in Fig. 9 to $(P)_T = 0$

TABLE III Mean tensile strength of fibres (test length 25 mm)

Fibre	Carbon			Polyarylate			
	C-1	C-2	C-3	V-1	V-2	V-3	V-4
Mean tensile strength							
Measured value (GPa)	3.28	2.59	2.23	3.93	3.48	3.34	3.63
Calculated value (GPa)	3.35	2.52	2.33	3.97	3.50	3.46	3.65

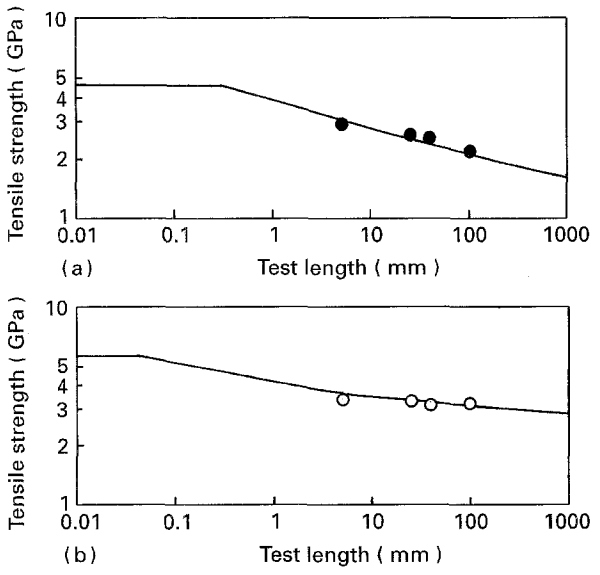

Figure 3 Relation between test length and tensile strength. (a) Graphitized fibre (C-2), (b) polyarylate fibre (V-3).

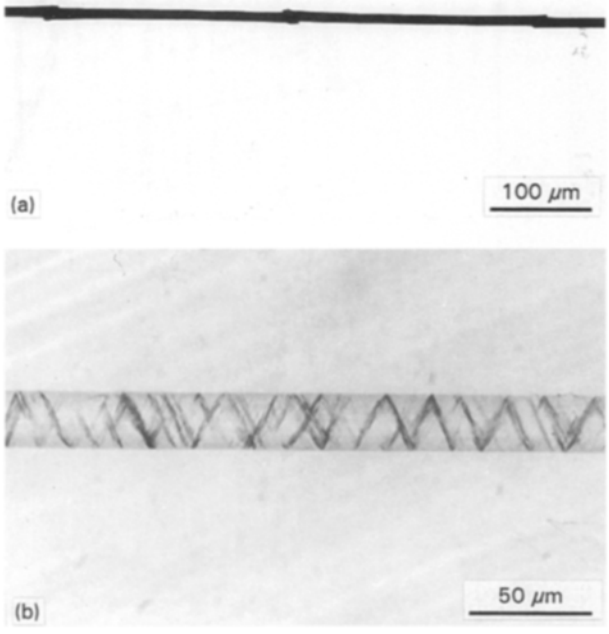

Figure 4 Photographs of fibre breaking points in the compression test (at 40° C). (a) Graphitized fibre (C-2), (b) polyarylate fibre (V-3).

as the real compressive strength of graphitized and polyarylate fibres and have shown the relationship between those values and fibre diameter in Fig. 10. With these fibres, the compressive strength increases with increasing fibre diameter. It is conceivable that the compressive strength of brittle fibres decreases with increasing fibre diameter due to a higher probability of flaws, in the same manner as the tensile strength, i.e. it has been confirmed that the compressive strength of graphitized and polyarylate fibres is variable with fibre size.

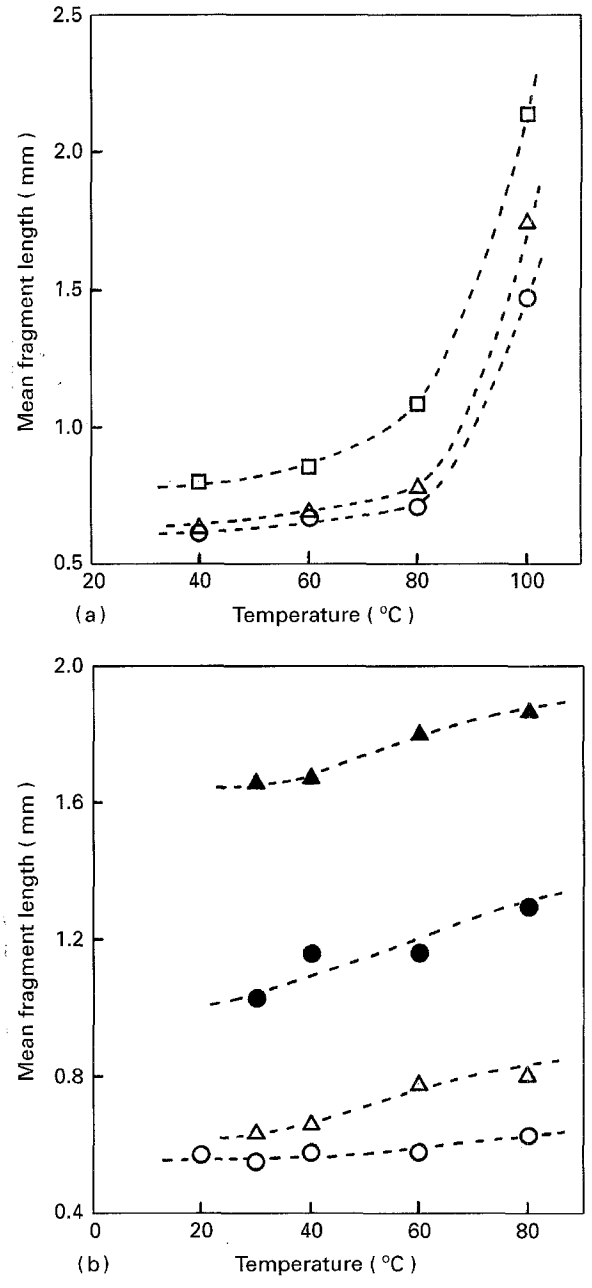

Figure 5 Relation between temperature and mean fragment length in tension. (a) Graphitized fibre, (○) C-1, (△) C-2, (□) C-3; (b) polyarylate fibre, (○) V-1, (△) V-2, (●) V-3, (▲) V-4.

The compressive strength of a graphitized fibre increases gradually with decreasing fibre diameter and remains almost unchanged at a diameter range smaller than 10 μm. On the other hand, the compressive strength of polyarylate fibre increases monotonically with decreasing fibre diameter within the fibre diameter range of this experiment. Assuming the increase in compressive strength is gradual at a diameter range smaller than 10 μm for the graphitized fibre, a similar tendency will also be expected for the polyarylate fibre. Accordingly, in order to obtain reinforcing fibres having a higher compressive strength, it will be necessary to prepare fibres having a diameter smaller than 10 μm.

In comparison with the compressive strength of pitch-based graphitized fibres, the compressive strength of polyarylate fibres is approximately one-tenth and is very low. The compressive strength of

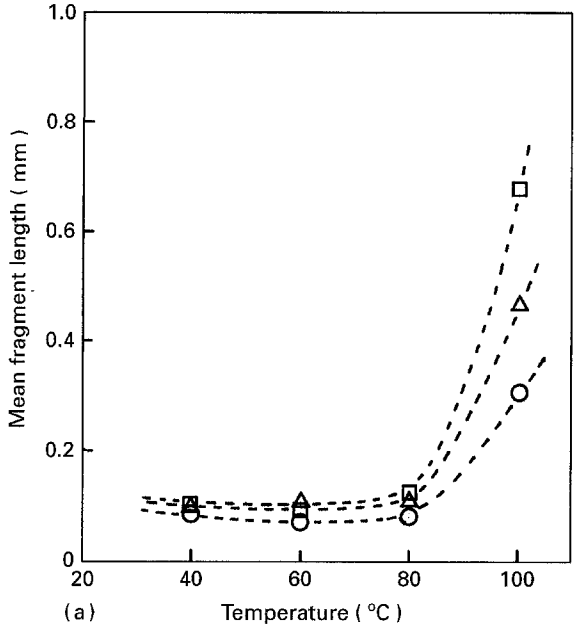

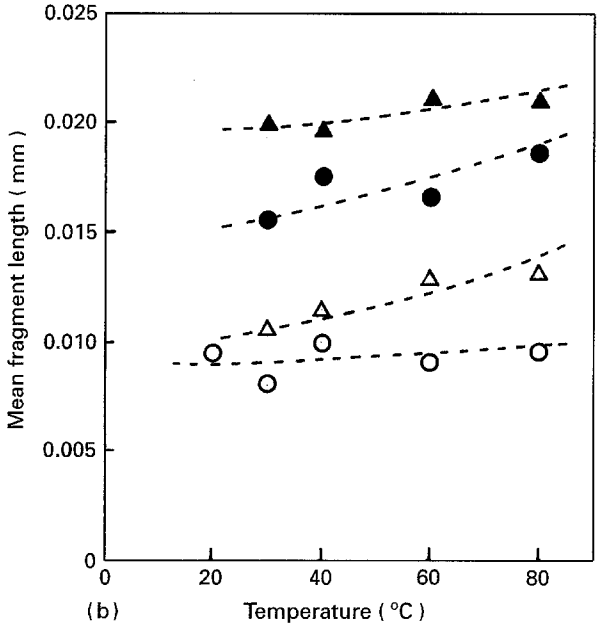

Figure 6 Relation between temperature and mean fragment length in compression. (a) Graphitized fibre, (○) C-1, (△) C-2, (□) C-3; (b) polyarylate fibre, (○) V-1, (△) V-2, (●) V-3, (▲) V-4.

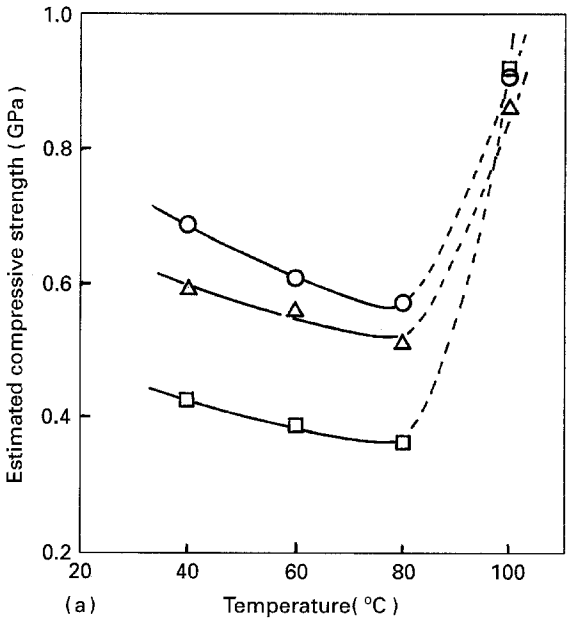

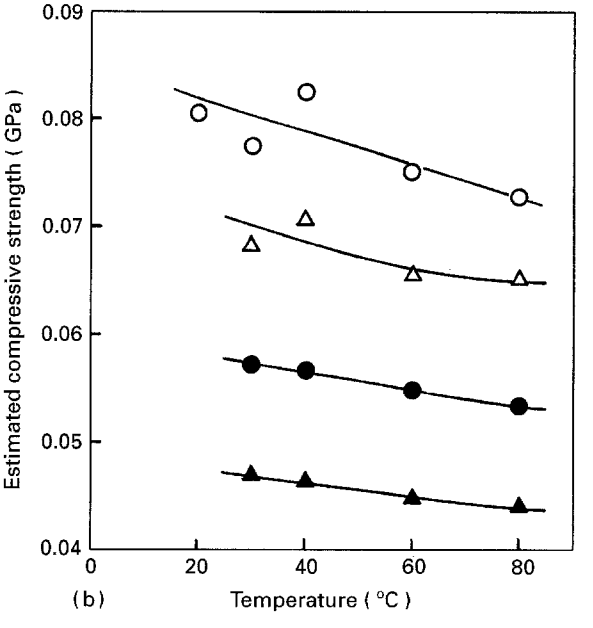

Figure 7 Relation between temperature and estimated mean compressive strength. (a) Graphitized fibre, (○) C-1, (△) C-2, (□) C-3; (b) polyarylate fibre, (○) V-1, (△) V-2, (●) V-3, (▲) V-4.

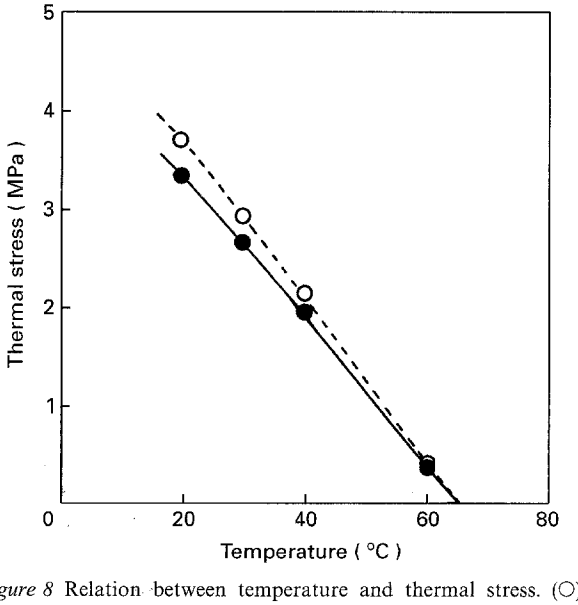

Figure 8 Relation between temperature and thermal stress. (○) Graphitized fibre-epoxy resin system, (●) polyarylate fibre-epoxy resin system.

graphitized fibre obtained in this experiment agrees well with a pitch-based graphitized fibre (0.65 GPa) (10 μm in diameter) as reported previously [29]. This indicates that the values of compressive strength obtained in this experiment are appropriate, and the reproducible value of compressive strength can be obtained by the above-mentioned method.

The compressive strength of polyarylate fibre is slightly lower than an aramid fibre (0.09 GPa) (Kevlar 29, higher strength type, 12.9 μm diameter) as reported previously [28].

4. Conclusion

If a sufficiently long fibre is embedded in the neighbourhood of the surface of a rectangular beam, and the system is subjected to a tensile (or compressive) strain greater than the fibre's ultimate strain according

TABLE IV Properties of epoxy resin at various temperatures

	20 °C	30 °C	40 °C	60 °C	80 °C
Young's modulus (GPa)	1.69	1.68	1.67	1.43	0.11
Thermal expansion coefficient (10^{-5} °C^{-1})	6.1	6.7	7.2	8.1	14.3
Poisson's ratio	0.30	0.32	0.33	0.35	0.38

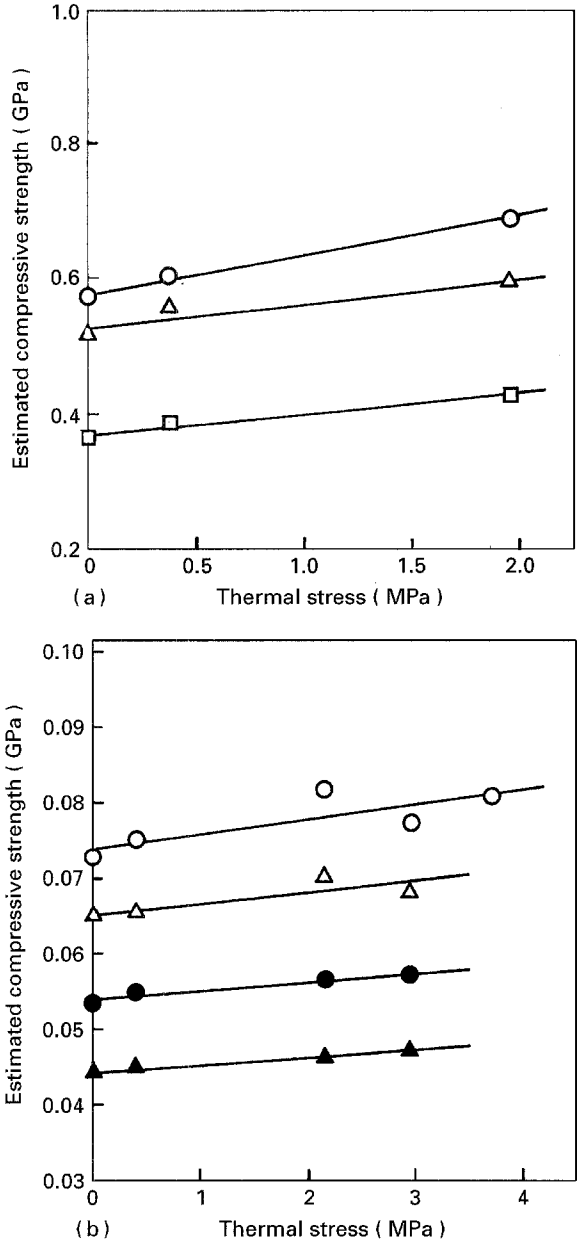

Figure 9 Relation between thermal stress and estimated mean compressive strength. (a) Graphitized fibre, (○) C-1, (△) C-2, (□) C-3; (b) polyarylate fibre, (○) V-1, (△) V-2, (●) V-3, (▲) V-4.

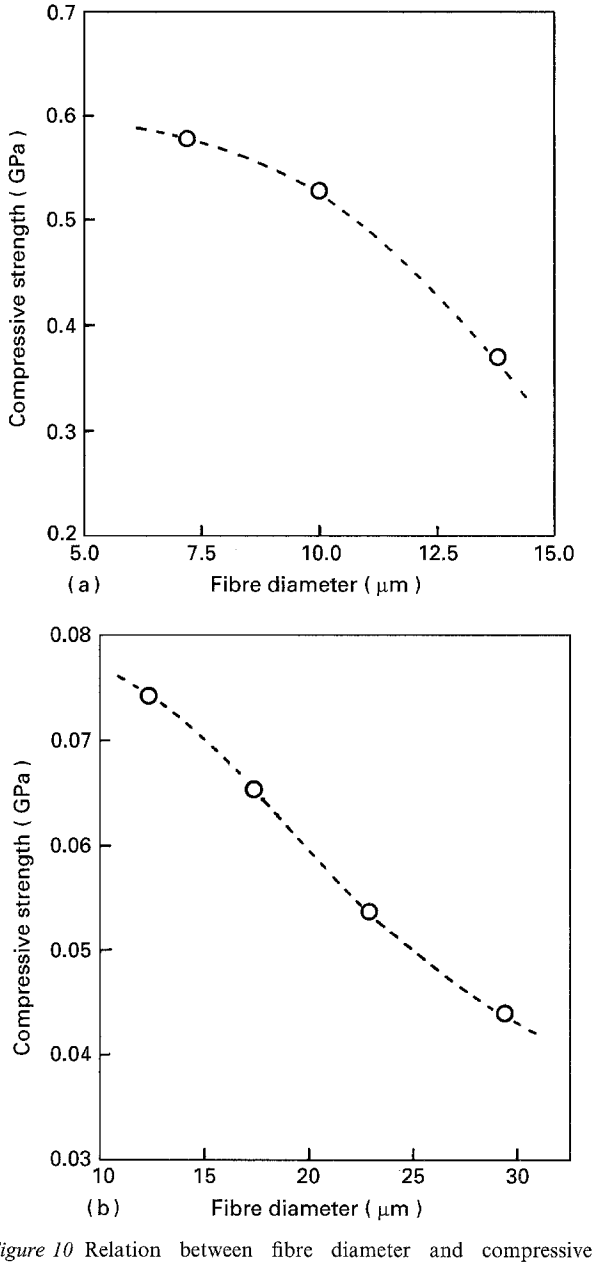

Figure 10 Relation between fibre diameter and compressive strength. (a) Graphitized fibre, (b) polarylate fibre.

to the bending method, the fibre eventually breaks into many pieces. By measuring the lengths of broken pieces and estimating the mean tensile strength from the length just before the final fragment length in tension, attempts were made to estimate the fibre axial compressive strength of pitch-based graphitized and polyarylate fibres, and the relationship between the compressive strength and fibre diameter was investigated.

The estimated compressive strength of fibres decreases with increasing temperature. This decrease in compressive strength may be accounted for by a decrease in the radial compressing force owing to a decrease in the residual thermal stress and a decrease in Young's modulus of the resin matrix.

There is a linear relationship between the estimated compressive strength and radial compressing force in a temperature range from room temperature to 80 °C. The real compressive strength of the fibres,

determined by extrapolating this straight line until the radial compressing force is zero, increases with decreasing fibre diameter, but remains almost unchanged at a diameter range smaller than 10 μm. In order to obtain reinforcing fibres having higher compressive strength, it will be necessary to prepare fibres having a diameter smaller than 10 μm.

Acknowledgements

We thank the Carbon Fibre Project Group, Corporate Research and Development Laboratory, Tonen Co. Ltd, and the Plastics Development and Technology Department, Kuraray Co. Ltd, for their financial contribution and the supply of the reinforcing fibres. Thanks are also due to Mr J. Takayasu, Mr E. Tsushima (Tonen), and Mr A. Mutoh, for useful comments and discussions.

References

1. D. SINCLAIR, *J. Appl. Phys.* **21** (1950) 380.
2. M. M. SCHOPPEE and J. SKELTON, *Text. Res. J.* **44** (1974) 968.
3. J. H. GREENWOOD and P. G. ROSE, *J. Mater. Sci.* **9** (1974) 1809.
4. M. G. DOBB, D. J. JOHNSON and B. P. SAVILLE, *Polymer* **22** (1981) 960.
5. S. J. DETERESA, S. R. ALLEN, R. J. FARRIS and R. S. PORTER, *J. Mater. Sci.* **19** (1984) 57.
6. S. J. DETERESA, R. S. PORTER and R. J. FARRIS, *ibid.* **20** (1985) 1645.
7. *Idem, ibid.* **23** (1988) 1886.
8. N. MELANITIS and C. GALIOTIS, *ibid.* **25** (1990) 5081.
9. S. J. DETERESA, *Carbon* **29** (1991) 397.
10. C. VLATTAS and C. GALIOTIS, *Polymer* **32** (1991) 1788.
11. W. C. DALE and E. BAER, *J. Mater. Sci.* **9** (1974) 369.
12. I. M. ROBINSON, P. H. J. YEUNG, C. GALIOTIS, R. J. YOUNG and D. N. BATCHELDER, *ibid.* **21** (1986) 3440.
13. R. L. KELLER and A. N. PALAZOTTO, "Collected Technical Papers AIAA/ASCE/ AHS", 28th Structural Dynamic Materials Conference (1987), Part 1 (1987) p. 245.
14. L. DRZAL, Air Force Wright Aeronautical Laboratories (AFWAL), Technical Report 86–4003 (1986).
15. S. R. ALLEN, *J. Mater. Sci.* **22** (1987) 853.
16. M. G. DOBB, D. J. JOHNSON and C. R. PARK, *ibid.* **25** (1990) 829.
17. F. J. McGARRY and J. E. MOALLI, *Polymer* **32** (1991) 1811.
18. A. S. ABHIRAMAN, AD Rep. (1992) 82.
19. H. JIANG, A. S. ABHIRAMAN and K. TSUI, *Carbon* **31** (1993) 887.
20. J. H. GREENWOOD and P. G. ROSE, *J. Mater. Sci.* **9** (1974) 1809.
21. N. L. HANCOX, *J. Mater. Sci.* **10** (1975) 234.
22. R. E. WILFONG and J. ZIMMERMAN, *J. Appl. Polym. Sci. Appl. Polym Symp.* **31** (1977) 1.
23. S. KUMAR and T. E. HELMINIAK, *Mater. Sci. Eng. Rigid-Rod Polymer Mater. Res. Soc. Symp. Proc.* **134** (1989) 363.
24. *Idem. SAMPE J.* **26** (1990) 51.
25. S. KUMAR, *Int. SAMPE Symp. Exhib.* **35** (1990) 2224.
26. M. MIWA, T. OHSAWA, M. KAWADE and E. TSUSHIMA, *Reinf. Plastics Jpn* **35** (1989) 199.
27. T. OHSAWA, M. MIWA, M. KAWADE and E. TSUSHIMA, *J. Appl. Polym. Sci.* **39** (1990) 1733.
28. M. MIWA, A. TAKENO and Y. LIU, *Reinf. Plastics Jpn* **37** (1991) 289.
29. M. MIWA, E. TSUSHIMA and J. TAKAYASU, *J. Appl. Polym. Sci.* **43** (1991) 1467.
30. M. MIWA, A. TAKENO, Y. LIU, A. WATANABE, J. TAKAYASU and E. TSUSHIMA, *Reinf. Plastics Jpn* **38** (1992) 433.
31. M. MIWA, T. OHSAWA and K. TAHARA, *Sen-i Gakkaishi* **35** (1978) T-19.
32. M. MIWA, T. OHSAWA and A. TOMITA, *Koubunshi Ronbunshu* **41** (1984) 353.
33. G. GERARD and A. C. GILLBERT, *J. Appl. Mech. (ASTM)* **24** (1957) 355.
34. A. KOBAYASHI, "20th Air Plane Symposium", Japan (1982) p. 70.
35. J. THEBERGE, J. CROSBY and M. HUTCHIUS, "40th Annual Conference, Reinforced Plastic/Composites", (SPI, 1985), Session 4-c.

Received 31 May 1994
and accepted 24 May 1995